

Experimental entangled photon pair generation using parallel crystals

Aitor Villar,¹ Alexander Lohrmann,¹ and Alexander Ling^{1,2}

¹*Centre for Quantum Technologies, National University of Singapore, 3 Science Drive 2, S117543*

²*Physics Department, National University of Singapore, 2 Science Drive 3, S117542*

(Dated: July 8, 2022)

We present an optical design where polarization-entangled photon pairs are generated within two β -Barium Borate crystals whose optical axes are parallel. This design increases the spatial mode overlap of the emitted photon pairs enhancing single mode collection without the need for additional spatial walk-off compensators. The observed photon pair rate is at least 65 000 pairs/s/mW with a quantum state fidelity of $99.37 \pm 0.13\%$ when pumped with an elliptical spatial profile.

Photon pair sources based on spontaneous parametric down-conversion (SPDC) are a standard tool in quantum optics when utilizing entanglement^{1–3}. The SPDC process takes place in the presence of a nonlinear crystal where a pump photon (p) can, under conservation of energy and momentum, spontaneously split into two strongly correlated lower energy photons (signal, s ; idler, i)⁴. Significant effort has been devoted towards developing bright entangled photon pair sources and a variety of source designs have been reported utilizing both critical^{5–8} and non-critical phase-matching techniques^{9,10}. Increasingly such light sources are being deployed outside the laboratory^{11–14} where environmental considerations play a role in the selection of phase-matching technique.

Non-critical phase-matching provides the brightest photon pair sources by providing access to a large nonlinearity¹⁵ and longer interaction lengths due to the absence of spatial walk-off^{10,16} while requiring very good temperature stability and often uses interferometric designs. When such requirements (such as temperature stability) cannot be met, critical phase-matching (CPM), where the tilt angle of the crystal optical axis is used to fulfill the momentum conservation, can be applied.

A common feature in all source designs based on CPM-SPDC using bulk crystals is the spatial walk-off that any light polarized parallel to the crystal optical axis (extraordinary) will undergo. This effect becomes paramount when the source consists of more than one crystal for entangled light generation (typically, when using type-I CPM). This spatial displacement eventually restricts the final mode overlap of SPDC emission coming from multiple nonlinear crystals. The standard source geometry in this case is the so-called *crossed-crystal* configuration comprising of two nonlinear crystals whose optical axes are rotated 90° with respect to each other^{6,8,17}.

In type-I phase-matching ($e_p \rightarrow o_s o_i$; e : extraordinary, o : ordinary) this crossed-crystal configuration can be used to create the maximally entangled Bell states. Furthermore, it allows both collinear or non-collinear emission, while the wavelengths can be readily tuned. However, the fact that each crystal yields a pump walk-off in orthogonal planes (vertically and horizontally) results in a non-optimal spatial overlap of the two SPDC modes. Entangled light can only be collected from the region of

optimum overlap, requiring additional birefringent crystals for spatial walk-off compensation. In addition to the spatial mismatch of the SPDC modes, the effective pump power is limited as the two crystals need to be pumped with orthogonal polarization components.

We present a polarization entangled photon pair source using collinear type-I CPM uniaxial crystals whose optical axes are parallel. This *parallel-crystal* configuration improves the spatial overlap of the target SPDC modes emerging from the two crystals. This is achieved by taking advantage of the characteristic walk-off in birefringent crystals so that the SPDC emission is self-compensated. This relaxes the alignment requirements while improving the overall rate of detection for entangled photon pairs. Furthermore, the source design uses fewer birefringent elements reducing the physical footprint.

The source design presented in this work avoids the characteristic drawbacks of the crossed-crystal source (lower effective pump power and two-dimensional walk-off) by using two crystals with parallel-aligned optical axes, as shown in Fig. 1(a). This allows both crystals to utilize the full pump power in the SPDC process. As the photon pairs in both crystals are generated in the same polarization state ($|H_s H_i\rangle$), the SPDC pairs from the first crystal need a 90° polarization rotation to achieve the desired quantum state,

$$|\Phi^\pm\rangle = \frac{1}{\sqrt{2}} (|H_s H_i\rangle \pm e^{i\Delta\Phi} |V_s V_i\rangle).$$

To realize this an achromatic half-wave plate is inserted in between the two crystals. This half-wave plate is designed to have no effect on the pump polarization. When the pump light travels through both crystals it undergoes walk-off in the vertical direction. Similarly the SPDC photons from the first crystal walk off in the same direction when traversing the second crystal.

As depicted in Fig. 1(a) this crystal configuration reduces the necessity of any additional spatial compensation crystals since the photon pairs emitted from both crystals overlap significantly in the same plane when exiting the second crystal (red and green ellipses). Note that the walk-off is a function of the wavelength and the crystal angle cut. In our experimental design using a pump

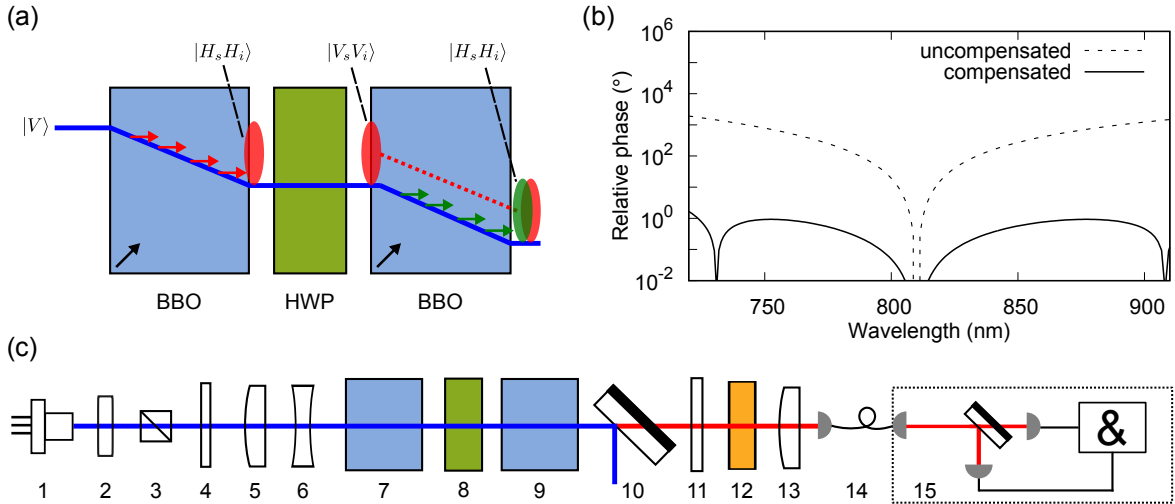


FIG. 1. Schematic for the source design. (a) Spatial self-compensation of the emitted photon pairs. The BBO optical axes are both pointing upwards as indicated by the black arrow. SPDC light is created along the pump path in both crystals and the red (green) ellipse indicates the shape of the SPDC emission generated in the first (second) BBO crystal. An achromatic half-wave plate rotates the polarization of the photons born in the first BBO. (b) Relative phase between $|V_s V_i\rangle$ and $|H_s H_i\rangle$ with (solid line) and without (dashed line) the phase compensation crystal. For BBO length of 5 mm, a YVO_4 length of 3.12 mm can act as the compensator. (c) Overview over the experimental setup, 1: laser diode, 2: fluorescence filter, 3: Glan-Taylor polarizer, 4: half-wave plate, 5: convex lens, 6: concave lens, 7: BBO, 8: achromatic half-wave plate, 9: BBO, 10: dichroic mirror, 11: long-pass filter, 12: phase compensation crystal, 13: collection lens, 14: single-mode fiber, 15: photon separation via a dichroic mirror followed by coincidence detection.

wavelength of 405 nm and β -Barium Borate (BBO) crystals with an angle cut of 28.8° , the walk-off introduces a 6% mismatch of the photon pair emission along the vertical direction, independent of crystal length. If necessary, this mismatch can be compensated by using a single birefringent crystal but is deemed sufficiently small in this work and neglected. Due to the spatial self-compensation and the maximal use of the pump power in both crystals, the parallel crystal configuration promises a significant increase in brightness over the traditional crossed-crystal configuration.

In order to observe a Bell state, the relative phase $\Delta\Phi$ between photon pairs generated in the first and second BBO crystals should have a negligible wavelength dependence^{8,18}. Photon pairs generated in the first (second) crystal will accumulate a phase Φ_1 (Φ_2) as they travel through the dispersive medium. The contribution to Φ_1 arises from the photon pairs traveling through the half-wave plate and the second BBO crystal. Additionally, it should be noted that these photon pairs have extraordinary polarization after the half-wave plate (HWP). The contribution to Φ_2 is similar to Φ_1 but differs where the phase through the first BBO crystal and the half-wave plate is picked up by the parent photon.

Without any additional birefringent elements, the relative phase will show a strong wavelength dependence. This wavelength dependence can be suppressed by the addition of an a-cut single yttrium orthovanadate crystal (YVO_4) with the correct orientation and length (3.12 mm in our case). Therefore $\Delta\Phi$ can be calculated with the

following equation,

$$\begin{aligned} \Delta\Phi &= \Phi_1 - \Phi_2, \\ \Phi_1 &= \phi_s^{\text{HWP}} + \phi_i^{\text{HWP}} + \phi_s^{\text{BBO}} + \phi_i^{\text{BBO}} + \phi_s^{\text{YVO}_4} + \phi_i^{\text{YVO}_4}, \\ \Phi_2 &= \phi_p^{\text{BBO}} + \phi_p^{\text{HWP}} + \phi_s^{\text{YVO}_4} + \phi_i^{\text{YVO}_4}. \end{aligned}$$

Due to the narrow bandwidth of the pump laser used in this work (≤ 160 MHz) all terms containing pump photons can be treated as a constant.

The relative phase is first evaluated without the phase compensation crystal to show strong wavelength-dependence (Fig. 1(b), dashed line). For clarity, the constant offset at the degenerate wavelength (810 nm) was subtracted. After adding the phase compensation crystal, the relative phase shows a negligible wavelength dependence (Fig. 1(b), solid line). With this amount of compensation, the maximally entangled state $|\Phi^-\rangle = (|H_s H_i\rangle - |V_s V_i\rangle)/\sqrt{2}$ can be achieved.

The experimental setup is shown in Fig. 1(c). Collimated light from a grating stabilized laser diode with a central wavelength of 405 nm was used to pump the nonlinear medium. Undesirable pump spectral components were removed by a fluorescence filter. The pump polarization state was prepared by a Glan-Taylor polarizer and a half-wave plate. In principle, these polarizing elements are not necessary as the laser output is highly polarized.

The pump beam has an elliptical spatial profile, with the major axis aligned in the walk-off direction. The ratio of the major and minor axes was 2:1. The pump focus (along the minor axis) was set in between the two 5 mm

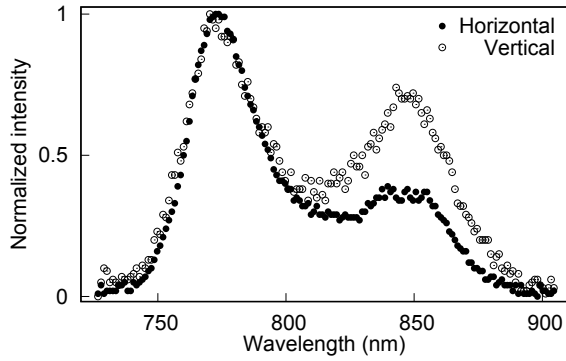


FIG. 2. Spectra for horizontally (black) and vertically (white) polarized photons. Resolution of the spectrometer: 2 nm. The intensity mismatch of the idler peaks for the two different polarization states is due to the polarization dependence of the spectrometer used.

thick crystals. The full-width half-maxima of the pump beam at the focus were 133:63 μm while the target signal and idler wavelengths were centred on 776 nm and 847 nm, respectively. A tailored achromatic half-wave plate rotates the polarization of the SPDC photons generated in the first crystal, while the pump polarization remains unaffected. Dichroic mirrors remove the excess pump.

The photon pairs were collected into a single-mode fiber (SMF) using an achromatic collection lens. The collection mode full-width half-maximum was set at 53 μm to enhance coupling efficiency. The collected photon pairs were split with respect to their wavelengths using a dichroic mirror, and guided into passively-quenched avalanche photodiodes (APDs) capable of single-photon detection. The single photon detection events from two APDs were checked for timing correlations using a coincidence time window set at 4 ns.

The entangled photon pair rate was measured without additional interference or polarization filters and a pump power of 0.1 mW was used to remain within the linear detection regime of the single-photon detectors. The normalized detected pair rate was 65 000 pairs/s/mW. In comparison to the brightest reported CPM crossed-crystal source (27 000 pairs/s/mW)⁸ using similar detector efficiencies, this corresponds to a 2.4 times increase in brightness. This improvement was achieved despite using crystals that were only one-third in length.

The heralding efficiency after subtracting for dark counts, was $27 \pm 1.0\%$ and $22.0 \pm 1.0\%$ for signal and idler photons, respectively. Spectral information of the SPDC photons is shown in Fig. 2.

To establish the presence of polarization entanglement it is necessary to observe the correlations in at least two polarization bases. We test the correlations using a single polarization analyzer placed after the phase compensation crystal. The use of a single polarization element to perform partial tomography is not common in the literature; it is appropriate in this work because the photons

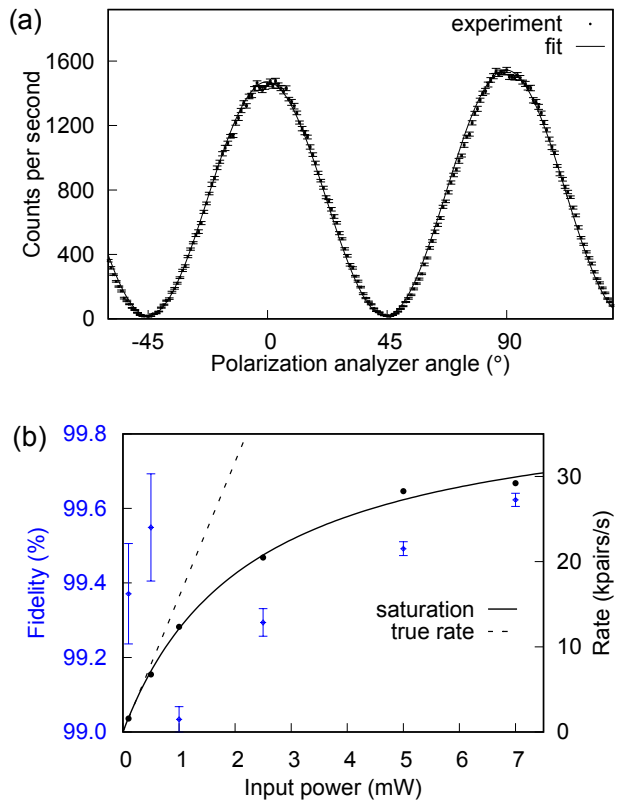


FIG. 3. (a) Correlation function obtained from a single polarization analyzer at a pump power of 0.1 mW. The peak at 0 (90) degree corresponds to horizontal (vertical) polarization. The fidelity calculated from the fit was $99.37 \pm 0.13\%$. (b) Power dependence of the fidelity (blue, left axis) and the detected pair rate (black, right axis) with the polarization analyzer in place. This source begins to saturate the passively-quenched detectors at 2 mW of pump power.

are always co-polarized in one basis ($H\backslash V$), while anti-polarized in the other linear basis. As the polarization analyzer is rotated the measurement transitions between the bases and the correlations for the state Φ^- will oscillate between maxima and minima. Phase-matching prevents the generation of $|H_sV_i\rangle$ or $|V_sH_i\rangle$ pairs in our design. Under this constraint, any possible mismatch between the measured state and Φ^- can be attributed to either a mixing with the Φ^+ state due to imperfect phase compensation, to an imbalance between the components $|H_sH_i\rangle$ and $|V_sV_i\rangle$, or to the collection of spatially distinguishable photons. Based on these assumptions, a measurement operator can be constructed to fit the experimentally observed data and to extract the Bell state fidelity, $F(\psi, \Phi^-) = \text{Tr}(\sqrt{\sqrt{\psi}\Phi^-\sqrt{\psi}})$.

The correlation curve was measured and is presented in Fig. 3(a). From this correlation curve a Bell state fidelity of $99.37 \pm 0.13\%$ was extracted. Experiments that utilize such a high brightness source would not be limited by pump power but by detector performance. We show in Fig. 3(b) the passively-quenched detectors are saturated

with only 7 mW of pump power, while the quantum state fidelity remained above 99%.

It is noteworthy that high brightness, good collection efficiency and near-unit quantum state fidelity were reported when the source was pumped directly from a laser diode without any spatial filtering. One benefit of the elliptical pump mode is the increased utilisation of the pump power in the volume of the collection mode; this was done by roughly matching the pump mode size in the minor axis with the circular symmetric collection mode. An interesting possibility is that further improvements may be using an elliptical collection mode.

The use of pumps with an elliptical spatial profile has been neglected in the existing literature which has focused on circular symmetric pump modes^{19–21} (being guided mostly by arguments derived from the Boyd-Kleinman parameter). However, as the optical axes in crystals suitable for SPDC are non-isotropic, non-circular pump profiles may also be suitable for high performance entangled light sources. Following this line of argument, one hypothesis to be tested is whether elliptical pump profiles are also useful for enhancing photon pair sources utilizing non-critical phase-matching. From a practical

perspective, the ability to forego spatial mode filtering for the pump increases the power available.

Work is ongoing to identify the optimal crystal lengths and beam parameters for achieving higher brightness. One direction is to investigate whether brightness and entanglement quality are conserved when the emitted photon pairs are collected into a field stop instead of a single-mode fiber. The combination of field stop collection with direct pumping from a laser diode without spatial filtering could lead to a new class of bright entangled light sources useful in both fundamental science and downstream applications.

ACKNOWLEDGMENTS

This research is supported by the National Research Foundation, Prime Ministers Office, Singapore under its Competitive Research Programme (CRP Award No. NRF-CRP12-2013-02). This program was also supported by the Ministry of Education, Singapore. The use of a single polarizing element for partial tomography was first suggested by W. Morong.

[1] T. E. Kiess, Y. H. Shih, A. V. Sergienko, and C. O. Alley, *Physical Review Letters* **71**, 3893 (1993).

[2] D. Bouwmeester, J.-W. Pan, K. Mattle, M. Eibl, H. Weinfurter, and A. Zeilinger, *Nature* **390**, 575 (1997).

[3] T. Jennewein, C. Simon, G. Weihs, H. Weinfurter, and A. Zeilinger, *Physical Review Letters* **84**, 4729 (2000).

[4] D. C. Burnham and D. L. Weinberg, *Physical Review Letters* **25**, 84 (1970).

[5] P. G. Kwiat, K. Mattle, H. Weinfurter, A. Zeilinger, A. V. Sergienko, and Y. H. Shih, *Physical Review Letters* **75**, 4337 (1995).

[6] P. G. Kwiat, E. Waks, A. G. White, I. Appelbaum, and P. H. Eberhard, *Physical Review A* **60**, R773 (1999).

[7] C. Kurtsiefer, M. Oberparleiter, and H. Weinfurter, *Physical Review A (Atomic, Molecular, and Optical Physics)* **64**, 023802 (2001).

[8] P. Trojek and H. Weinfurter, *Applied Physics Letters* **92**, 211103 (2008).

[9] T. Kim, M. Fiorentino, and F. N. Wong, *Physical Review A* **73**, 012316 (2006).

[10] F. Steinlechner, S. Ramelow, M. Jofre, M. Gilaberte, T. Jennewein, J. P. Torres, M. W. Mitchell, and V. Pruneri, *Optics express* **21**, 11943 (2013).

[11] I. Marcikic, A. Lamas-Linares, and C. Kurtsiefer, *Applied Physics Letters* **89**, 101122 (2006).

[12] R. Ursin, F. Tiefenbacher, T. Schmitt-Manderbach, H. Weier, T. Scheidl, M. Lindenthal, B. Blauensteiner, T. Jennewein, J. Perdigues, P. Trojek, B. mer, M. Frst, M. Meyenburg, J. Rarity, Z. Sodnik, C. Barbieri, H. Weinfurter, and A. Zeilinger, *Nature Physics* **3**, 481 (2007).

[13] Z. Tang, R. Chandrasekara, Y. C. Tan, C. Cheng, L. Sha, G. C. Hiang, D. K. Oi, and A. Ling, *Physical Review Applied* **5**, 054022 (2016).

[14] J. Yin, Y. Cao, Y.-H. Li, S.-K. Liao, L. Zhang, J.-G. Ren, W.-Q. Cai, W.-Y. Liu, B. Li, H. Dai, *et al.*, *Science* **356**, 1140 (2017).

[15] F. Steinlechner, P. Trojek, M. Jofre, H. Weier, D. Perez, T. Jennewein, R. Ursin, J. Rarity, M. W. Mitchell, J. P. Torres, *et al.*, *Optics express* **20**, 9640 (2012).

[16] F. Steinlechner, M. Gilaberte, M. Jofre, T. Scheidl, J. P. Torres, V. Pruneri, and R. Ursin, *JOSA B* **31**, 2068 (2014).

[17] R. Rangarajan, M. Goggin, and P. Kwiat, *Optics express* **17**, 18920 (2009).

[18] Y.-H. Kim, S. P. Kulik, and Y. Shih, *Physical Review A* **62**, 011802 (2000).

[19] D. Kleinman, *Physical Review* **174**, 1027 (1968).

[20] A. Ling, A. Lamas-Linares, and C. Kurtsiefer, *Physical Review A* **77**, 043834 (2008).

[21] R. S. Bennink, *Physical Review A* **81**, 053805 (2010).